Influence of the nature and environment of cobalt on the catalytic activity of Co-BEA zeolites in selective catalytic reduction of NO with ammonia

Rafal Baran, Jean-Marc Krafft, Thomas Onfroy, Teresa Grzybek, Stanislaw Dzwigaj

Influence of the nature and environment of cobalt on the catalytic activity of Co-BEA zeolites in selective catalytic reduction of NO with ammonia

Rafal Baran[1,2,3], Jean-Marc Krafft[2,3], Thomas Onfroy[2,3],

Teresa Grzybek[1], Stanislaw Dzwigaj[2,3,*]

[1]Faculty of Energy and Fuels, AGH University of Science and Technology, Al. A. Mickiewicza 30, 30-059 Krakow, Poland

[2]Sorbonne Universités, UPMC Univ Paris 06, UMR 7197, Laboratoire de Réactivité de Surface, F-75005, Paris, France

[3]CNRS, UMR 7197, Laboratoire de Réactivité de Surface, F-75005, Paris, France

Figures: 10

Tables : 5

Keywords: Cobalt, BEA, postsynthesis, SCR of NO, NH_3

***Corresponding author:**

Dzwigaj Stanislaw, E-mail : stanislaw.dzwigaj@upmc.fr, tel : 33 1 44 27 21 13

Abstract

The influence of cobalt environment on the catalytic properties of Co_xSiBEA zeolite in selective catalytic reduction of NO with ammonia was studied. Catalysts were prepared by a two-step postsynthesis method which consists, in the first step, of dealumination of parent BEA zeolite to obtain aluminum-free SiBEA support and then, in the second step, of contacting the obtained material with an aqueous solution of cobalt nitrate. DR UV-Vis and XPS results showed that cobalt was successfully incorporated into zeolite beta framework as isolated mononuclear Co(II). The presence of only isolated framework mononuclear Co(II) was evidenced in Co_xSiBEA with cobalt content lower than 2 wt % and both isolated framework mononuclear Co(II) and extra-framework octahedral Co(II) for $Co_{3.0}$SiBEA catalyst. FTIR investigation of pyridine adsorption revealed that the incorporation of cobalt into zeolite framework led to a creation of new Lewis acidic sites which are responsible for high activity in SCR of NO with ammonia. The catalytic activity of Co_xSiBEA in selective catalytic reduction of NO with ammonia as reducing agent strongly depends on the nature and environment of cobalt in BEA structure. The single-site $Co_{2.0}$SiBEA zeolite catalyst was the most active among tested, with maximum NO conversion about 80 % at 673 K. In contrast, $Co_{3.0}$SiBEA catalyst containing a mixture of framework and extra-framework Co(II) had lower activity in SCR of NO process than $Co_{2.0}$SiBEA at higher temperature due to a competitive reaction of ammonia oxidation to NO.

1. Introduction

Despite of numerous publications and much scientific research on selective catalytic reduction of NO_x with ammonia [1–7] or hydrocarbons [8–11] as reducing agents, there is still a lot of questions about the reaction mechanism, as well as the formation of by-products as a result of competitive reactions of ammonia and hydrocarbons oxidation.

Moreover, improvements in currently used SCR technology are required. Another important factor from the point of view of industrial application in power plants and automotive engines is longtime catalyst stability and durability.

To obtain a very efficient catalyst for the removal of nitrogen oxides, excellent dispersion of active species is needed which will allow to hinder side reactions [12,13]. To achieve this, new methods of catalyst preparation should be developed because conventional ones result in the formation of different metal species. In the case of cobalt-containing zeolites isolated framework cobalt species, cobalt ions in ion-exchange positions, cobalt oxide clusters and crystallites and Co_3O_4 were found, depending on the conditions of preparation procedures [12,14,15].

Recent works on the application of cobalt-containing materials for selective catalytic reduction of NO_x with ammonia [16–19] or methane [20,21] gave promising results and established cobalt as an attractive active material for the removal of NO_x from exhaust gases, but further investigation of cobalt speciation and optimal loading should be carried out.

In our work we obtained single-site cobalt zeolite catalyst due to the application of two-step postsynthesis method which consists of the creation of a vacant T-atom sites with associated silanol groups by dealumination of parent beta zeolite by treatment with nitric acid, and the following incorporation of cobalt in the framework of resulting SiBEA zeolite by its reaction with silanol groups [22]. With the combined use of various spectroscopy techniques, we have proved the formation of isolated framework mononuclear Co(II).

The subject of this research was to study the influence of the nature and environment of cobalt present in Co-BEA zeolites on the selective catalytic reduction of NO with NH_3.

2. Experimental Section

2.1 Materials

The two type of zeolite BEA samples were prepared. First series of Co_xSiBEA catalysts was prepared by two-step postsynthesis procedure. In the first step, 2 g of parent TEABEA zeolite was treated with 0.2 L of nitric acid aqueous solution (13 mol L^{-1}) at 353 K for 4 hours in order to remove aluminum from zeolite framework. The obtained Al free SiBEA solid was washed several times with distilled water and dried overnight at 363 K.

In the second step, 2g of SiBEA zeolite was contacted with 0.2 L of cobalt nitrate solution with an appropriate concentration and kept for 24 hours under vigorous stirring. After this time the suspension was transferred into an evaporator and dried for two hours under vacuum pump. In this way, a set of zeolites was prepared and labeled: $Co_{1.0}$SiBEA, $Co_{2.0}$SiBEA and $Co_{3.0}$SiBEA, where the number following the element symbol stands for the weight percentage of introduced cobalt.

HAlBEA zeolite was prepared by conventional ion exchange of AlBEA with 0.1 mol L^{-1} ~~dm^{-3}~~ NH_4NO_3 solution following calcination of TEABEA for 15 h at 823 K as described earlier [23].

$Co_{2.0}$HAlBEA were obtained by conventional wet impregnation of 2 g of HAlBEA with appropriate concentration of aqueous $Co(NO_3)_2$ solution [24]. This sample was prepared as reference for Co_xSiBEA zeolites.

2.2. Apparatus and Procedures

X-ray Fluorescence chemical analysis was performed at room temperature on SPECTRO X-LabPro apparatus.

XRD analysis was carried out on a PANalitical Empyrean diffractometer using the CuK_α radiation (λ = 154.05 pm). All experiments were performed at room temperature. XRD relative crystallinity of the samples was calculated using the main diffraction reflex area form XRD patterns considering the TEABEA zeolite as 100 % crystalline.

Low temperature nitrogen sorption experiments were carried out on a Micromeretics ASAP 2010 apparatus. All samples were outgassed, first at room temperature, then at 623 K to a pressure lower than 0.2 Pa. The specific surface areas were determined using BET method. The microporous pore volume was determined from the amount of N_2 adsorbed up to $P/P_0 = 0.2$

FTIR spectra in transmission mode were registered on PerkinElmer Frontier spectrometer. The mixture of KBr and zeolite sample (200:1) was carefully ground and pressed into a wafer under pressure of 2 tons cm^{-2}. The framework vibrational spectra were recorded between 400 and 4000 cm^{-1} with a resolution of 4 cm^{-1}.

DR UV-vis experiments were carried out at ambient atmosphere on a Cary 5000 Varian spectrometer equipped with a double integrator with polytetrafluoroethylene as reference.

XPS measurements were carried out with Omicron (ESCA+) spectrometer, using an Al Kα (hν = 1486.6 eV) X-ray source equipped with a flood gun. The sample area used for analysis was 3 mm^2. Zeolite samples were pressed into an indium foil. Binding energy (BE) of Co, Si and O was calibrated to the Si 2p peak at 103.3 eV. Before analysis, the samples were degassed at room temperature to a pressure of 10^{-7} Pa. A number of components were determined with a Voigt function (a 70/30 composition of Gaussian and Lorentzian functions).

Infrared spectroscopy of CO adsorption/desorption experiments were performed on a Bruker Vertex 70 spectrometer. Before analysis, self supported samples were pressed at ca. 1 tons cm^{-2} into thin wafers of ca. 10 mg cm^{-2} and set inside the glass cell where they were pre-treated at 723 K for 2 h in flowing 2.5% O_2/Ar and then degassed at 573 K (10^{-3} Pa) for 1 h.

Finally, IR cell was cooled down to 100 K with liquid nitrogen, and CO was added in small portions up to an equilibrium pressure of 133 Pa. Then the sample was evacuated up to 10^{-3} Pa at room temperature. The spectra were obtained after subtraction of the spectrum recorded before CO adsorption.

The quantity of Brønsted and Lewis acidic sites was determined by adsorption of pyridine followed by infrared spectroscopy, using the parameters calculated by Emeis [25]. The samples were prepared in the same way as for the CO sorption experiments. The wafers activation procedure was performed as described before [22]. Bruker Vector 22 spectrometer (resolution 2 cm^{-1}, 128 scans) was used to record the spectra after desorption from 423 and 573 K for 1 h. The final spectra were obtained after subtraction of the spectrum recorded before pyridine adsorption from the spectrum recorded after pyridine adsorption.

The activity tests of cobalt containing catalysts in selective catalytic reduction (SCR) of NO with ammonia were performed in a fixed bed reactor. Temperature was measured inside the reactor with a thermocouple and controlled with an electronic controller (LUMEL RE19). The composition of the reaction gas was: 1000 ppm NO, 1000 ppm NH_3, 3.5 vol.% O_2 and He as balance. The gas mixture was provided with calibrated electronic mass flow controllers (BETA-ERG). The total gas flow was 0.1 L min^{-1} and catalyst mass was 0.2 g. The concentrations of NO and N_2O after reaction were analyzed by FTIR detectors (ABB 2020 AO series). Prior to the reaction the catalyst bed was activated in 3.5%O_2/He flow (0.1 L min^{-1}) in the temperature range of 298–798 K with a linear heating rate of 2 K min^{-1} and then for 1 h at 798 K. The standard test was carried out over 1 h at 573–773 K with increasing

reaction temperature every 50 K interval. The NO conversion was calculated from the measured concentration of nitric oxide.

Catalytic tests of ammonia oxidation were carried out in exactly the same way but without the presence of NO in the substrates stream.

3. Results and Discussion

3.1. Structural stability of Co_xSiBEA zeolites as evidenced by XRD and low temperature N_2 sorption

Table 1 exhibits the chemical composition of all samples mentioned in this work. The Si/Al ratio of the parent zeolites TEABEA was 17 and for dealuminated samples was higher than 1000. The final contribution of Co was very close to theoretical one, calculated before sample preparation.

The X-ray diffractograms of TEABEA, HAlBEA, $Co_{2.0}$HAlBEA, SiBEA, $Co_{2.0}$SiBEA and $Co_{3.0}$SiBEA catalysts are shown in **Figure 1.** All of them correspond to the pattern of zeolite beta structure [26,27]. As we reported before [23,28] shifts of narrow diffraction reflection located around 22.5 ^{o} are generally taken as evidence of lattice contraction or expansion. In the **Table 2** structural characteristic of BEA samples are collected. The position of the main diffraction peak increase from 22.326 ^{o} for TEABEA to 22.493 ^{o} for HAlBEA, and to 22.662 ^{o} for SiBEA indicating some relaxation of beta matrix related to removal of aluminum species form the framework. Introduction of cobalt into SiBEA zeolite led to the opposite shift of the main diffraction reflection from 22.662 ^{o} for SiBEA to 22.536 ^{o} for $Co_{2.0}$SiBEA and to 22.530° for $Co_{3.0}$SiBEA suggesting incorporation of cobalt into the framework of zeolite.

Diffractograms of the Co_xSiBEA recorded after SCR of NO with ammonia were almost identical of those before this reaction (result not shown), indicating that upon SCR

process the structure of the studied catalysts was not affected. No oxide phases were detected for spent-C-$Co_{2.0}$SiBEA and spent-C-$Co_{3.0}$SiBEA, confirming that sintering of cobalt species did not take place during the reaction.

As shown in **Table 3**, the textural properties of studied samples are typical for zeolite beta [29,30] and did not significant change neither over calcination for 15 hours at 823 K nor after treatment with nitric acid. Also formation of additional mesoporosity was not observed. Furthermore, the introduction of cobalt into SiBEA did not involve change of pore volume and specific surface area of zeolite.

An additional evidence of cobalt incorporation into the zeolite framework is strong modification of IR band at 950 cm^{-1} assigned to the stretching vibration of Si-O belonging to the uncoupled SiO_4 tetrahedra with a hydroxyl group, in line with earlier work on BEA zeolite [31–33].

As it is seen on **Figure 2,** FTIR spectra of parent TEABEA zeolite do not exhibit peak at around 950 cm^{-1} indicating absence of structural damages. Calcination of the parent zeolite led to the appearance of low intense bond at 950 cm^{-1} on HAlBEA spectrum and the treatment with nitric acid involve a considerable increase in the intensity of this band suggesting the formation of vacant T-atom sites, in agreement with earlier reports [31–33].

After the contacting of SiBEA with cobalt precursor (aqueous solution of $Co(NO_3)_2$) the significant decreasing of the intensity of FTIR band at 950 cm^{-1} was observed and new band at 955 cm^{-1} was appeared indicating reaction of Co precursor with silanol groups of vacant T-atom sites and incorporation of cobalt into zeolite framework.

3.2. Nature of cobalt in Co_xSiBEA zeolites as determined by DR UV-Vis and XPS

The DR UV−vis spectrum of the calcined $Co_{2.0}$SiBEA (C-$Co_{2.0}$SiBEA) zeolites (**Fig. 3**) exhibits two characteristic bands at 600 and 670 nm, ascribed to isolated framework

mononuclear Co(II), in agreement with the earlier reposts [34,35]. The DR UV-Vis spectrum of C-$Co_{3.0}$SiBEA catalyst containing 3.0 wt % of cobalt, besides the bands at 600 and 670 nm, contains an additional one at 510 nm, related to Co(II) species of octahedral coordination, in agreement with the earlier work on CoAPO-5 [36] and CoMOR [37] materials. Thus, for C-$Co_{3.0}$SiBEA catalyst, apart from the isolated framework mononuclear Co(II), extra-framework octahedral Co(II) may also be present, influencing its properties in the catalytic reaction.

DR UV–Vis spectrum of C-$Co_{2.0}$HAlBEA displays additional bond at 765 nm in comparison to C-$Co_{3.0}$SiBEA sample. This signal may be ascribed to oxygen-to-metal charge transfers for Co(III), in line with earlier studies for cobalt containing materials [38–40]. So, the presence of two types of Co(II) species in C-$Co_{2.0}$HAlBEA, first one as isolated mono-nuclear Co(II) and second one as polynuclear Co(II) in octahedral environment as well as Co(III) species is confirmed.

The XPS experiments were carried out in the BE ranges corresponding to O 1s, Si 2p, and Co 2p to elucidate the types of surface cobalt species present in Co_xSiBEA catalysts.

The XPS chemical composition of studied samples is summarized in Table 4. The Si/Al ration of C-$Co_{2.0}$HAlBEA is very similar to the one calculated from XRF experiments. The lower Co/Si ratio for all Co-containing samples may be due to very high dispersion of cobalt species in whole zeolite grains.

The XP spectrum of C-$Co_{1.0}$SiBEA zeolite was described recently in our work [22] and it reveals signals of Co $2p_{3/2}$ and Co $2p_{1/2}$ at 780.5 and 796.0 eV respectively, corresponding to cobalt present in the framework of BEA zeolite as isolated mononuclear Co(II), in line with the earlier reports on cobalt-containing zeolites [41,42]. The satellite peaks at 785.5 and 800.9 eV are the evidence of shake-up electrons typical for cobalt(II).

In comparison, XPS spectrum of C-$Co_{3.0}$SiBEA (**Fig. 4**) contains pair of peaks in both Co $2p_{3/2}$ and Co $2p_{1/2}$ ranges, suggesting the presence of two types of cobalt surface species.

Besides the peaks at 780.4 and 796.1 eV related to isolated framework mononuclear Co(II), additional ones at 781.7 and 797.7 eV appeared, which might be linked to octahedral Co(II) in extra-framework positions in agreement with the study on cobalt modified LTL zeolite [15].

XPS spectrum of C-$Co_{2.0}$HAlBEA zeolite reveals three values of BE of Co $2p_{3/2}$ and of Co $2p_{1/2}$ at 779.8, 781.3,784.2 eV and 795.9, 797.5, 800.3 eV, respectively. The values of Co $2p_{3/2}$ at 781.3 eV and of Co$2p_{1/2}$ at 797.5 eV may be assigned to very well dispersed extra-framework mononuclear Co(II), in line with earlier observations on Co-ZSM5 and Co-beta zeolites [35,43]

However, the second values of BE of Co $2p_{3/2}$ and Co $2p_{1/2}$ peaks at 784.2 and 800.3 eV, respectively, may be ascribed to polynuclear Co(II) [13,41]. Furthermore, the presence of additional peaks at 779.8 and 795.9 eV suggests the presence of Co(III). It indicates that some amount of Co(II) introduced into HAlBEA was oxidized to Co(III) over thermal treatment at 773 K in air.

3.4. The nature and strength of acidic centers as determined by FTIR of adsorbed pyridine and CO

Figure 5 displays the FTIR spectra of HAlBEA, $Co_{2.0}$HAlBEA, SiBEA, $Co_{2.0}$SiBEA and $Co_{3.0}$SiBEA after adsorption of pyridine at room temperature and the following desorption at 423 K for 1 hour.

The acidic properties of HAlBEA and $Co_{2.0}$HAlBEA were precisely describe in our earlier work [24]. HAlBEA contains large amount of strong Bronsted and Lewis acidic sites related to presence of Si–O(H)–Al groups and unsaturated Al(III) centers, respectively. Introduction of Co ions into HAlBEA leads to formation in $Co_{2.0}$HAlBEA additional amount

of Lewis acidic centers related to Co(II) and/or Co(III) species confirmed by appearance of intense bands at 1449 and 1611 cm^{-1}.

For SiBEA a very low amount of Brønsted and Lewis acidic centers was proven (**Table 5**) by the appearance of low bands at 1546 and 1638 cm^{-1} typical for pyridine cations, and at 1455 cm^{-1}, attributed to coordinatively bonded pyridine [28].

The introduction of cobalt into SiBEA led to the formation of high amount of Lewis acidic centers with a moderate strength, confirmed by the presence of high intense band at 1450 cm^{-1}, in line with a similar observation for NiSiBEA zeolite [44]. However, for $Co_{2.0}$SiBEA, the amount of acidic centers is higher than for $Co_{3.0}$SiBEA which may suggest that only Co incorporated into zeolite framework as isolated framework mononuclear Co(II) resulted in the creation of Lewis acidic centers, whereas the introduction of higher amount of cobalt led to the formation of extra-framework Co oligomers without further creation of Lewis acidic centers (**Table 5**). A lower amount of Lewis acidic centers determined by pyridine adsorption for $Co_{3.0}$SiBEA than for $Co_{2.0}$SiBEA may also be the result of blocking the access to the cobalt framework centers by Co oligomers located in the extra-framework positions of BEA zeolite. **Table 5** additionally shows changes in the concentration of acidic centers after recording the spectra at the different temperatures. For $Co_{2.0}$SIBEA and $Co_{3.0}$SiBEA zeolites, after increasing temperature from 423 to 573 K, a decrease in Lewis acidic centers concentration is about 38% and 42%, respectively, suggesting a moderate acidic strength of isolate framework mononuclear Co(II).

In order to characterize the nature of cobalt species and the strength of acidic centers in CoSiBEA, CO adsorption following FTIR experiments was carried out.

FTIR spectra of carbon monoxide adsorbed on activated $Co_{2.0}$SiBEA zeolite (**Fig. 6A**) exhibit five different bands in the carbonyl region at 2133, 2160, 2174, 2185 and 2215 cm^{-1}. The bands at 2160 and 2174 cm^{-1} are assigned to CO interacting with SiO-H group and

bridged Si-O(H)-Al, respectively, in line with earlier reports [23,45]. The latter appeared due to a small amount of framework aluminum remaining in SiBEA after treatment of TEABEA with nitric acid in the first step of the preparation procedure. According to the investigation of Hadjiivanov et al. on Co-ZMS-5 [46,47], and cobalt containing BEA zeolite [48] as studied by Mihaylova et al., the bands at 2185 and 2215 cm^{-1} are assigned to two types of monocarbonyl species formed after CO adsorption on the framework Co(II) species. Comparing the intensities of the two mentioned bands, the former cobalt species had much higher concentration. The remaining band at 2133 cm^{-1} is correlated with physically adsorbed CO molecules [7].

To describe the strength of hydroxyl groups present in $Co_{2.0}$SiBEA, the analysis of FTIR spectra in OH groups vibration range after CO sorption were performed.

The difference spectra (**Fig. 6B**) reveal four positive bands at 3653, 3435, 3345 and 3261 cm^{-1}, as well as one negative band at 3738 cm^{-1}. The FTIR band at 3738 cm^{-1} is attributed to internal silanol groups in line with earlier works [49]. The positive bands at 3653, 3435 and 3345 cm^{-1} appeared as the shift of bands related to internal SiO-H, AlO-H and acidic hydroxyl groups present in BEA zeolite, respectively, in agreement with earlier report [23].

A small shift from 3738 cm^{-1} to 3653 cm^{-1} (blue shift, 85 cm^{-1}) for the isolated silanol groups indicates that they posses very weak acidic character. The band at 3435 and 3345 cm^{-1} resulted from a shift of bands primarily located at 3660 and 3608 cm^{-1}, respectively. The considerable shifts of AlO-H (225 cm^{-1}) and Si-O(H)-Al (263 cm^{-1}) indicate a very strong acidic character of both Lewis and Brønsted centers. However, because of low intensity of these bands, a very low concentration of acidic centers related to aluminum sites is confirmed in $Co_{2.0}$SiBEA catalyst.

Fig. 7A shows the changes in the carbonyl region after gradual evacuation. The first bands present at 2140 and 2133 cm^{-1}, which disappeared upon outgassing, correspond to very weakly coordinated CO. Then 2160 cm^{-1} band was removed, indicating weak interactions between silanol groups and carbon monoxide. Further evacuation led to a partial disappearance of the bands at 2174, 2215 and 2185 cm^{-1}. These results show that the most stable interactions occurred between CO and acidic hydroxyls, as well as cobalt(II), confirming strong acidic character of both species.

Similar conclusion may be drawn after the analysis of hydroxyl region of the spectra recorded on gradually evacuated $Co_{2.0}$SIBEA sample (**Fig. 7B**). The first band which disappeared is that at 3660 cm^{-1}, confirming very low acidic strength of SiO-H groups. The bands at 3379 and 3257 cm^{-1} related to aluminum species forming strong Lewis and strong Brønsted acidic centers, remained the longest during outgassing of $Co_{2.0}$SiBEA sample.

3.5. Catalytic activity of Co_xSiBEA zeolites

The $Co_{1.0}$SiBEA, $Co_{2.0}$SiBEA, $Co_{3.0}$SiBEA and $Co_{2.0}$HAlBEA zeolites were tested in selective catalytic reduction of NO with ammonia. SCR reaction on cobalt containing catalyst goes according to following scheme:

$$4NH_3 + 4NO + O_2 = 4N_2 + 6H_2O \qquad (1)$$

However, often secondary reaction

$$4NH_3 + 4NO + 3O_2 = 4N_2O + 6H_2O \qquad (2)$$

or competitive ammonia oxidation reactions

$$2NH_3 + 2O_2 = N_2O + 3H_2O \qquad (3)$$

$$4NH_3 + 5O_2 = 4NO + 6H_2O \qquad (4)$$

$$4NH_3 + 3O_2 = 2N_2 + 6H_2O \qquad (5)$$

occur due to non-selectivity of the applied Co-catalysts, resulting in the formation of different kinds of Co(II) and Co(III) species, thus leading to low efficiency, especially at high temperature range [12,16,19].

NO conversion for Co_xSiBEA is presented in **Figure 8**. SiBEA support showed very low activity in the whole temperature range. Maximum NO conversion was achieved at 623 and 673 K and did not exceed 15 %. The application of catalysts containing cobalt species resulted in the increase in NO conversion. Depending on the cobalt content, different activity was achieved at a given temperature. $Co_{1.0}$SiBEA and $Co_{2.0}$SiBEA catalysts present a typical volcano-like activity in selective catalytic reduction of NO with ammonia. The highest activity for these catalysts was achieved at 623 – 723 K with the maximum NO conversion of 79% at 673 K for $Co_{2.0}$SiBEA catalyst. Such high activity is related to the presence of isolated framework mononuclear Co(II) whose presence was confirmed by XPS, DR UV-Vis and FTIR results.

In contrast, $Co_{3.0}$SiBEA catalyst behaved differently. For this catalyst, NO conversion quickly decreased with the increasing temperature from 50 % at 573 K to 4 % at 773 K. This behavior may be related to catalyst deactivation or competitive ammonia oxidation reactions. The similar behavior with the increasing of Co content was observed earlier for Co-ZSM-5 zeolites and cobalt containing mesoporous silica [12].

For $Co_{2.0}$HAlBEA catalyst, NO conversion increased with temperature and reached maximum of 65% at 773 K. Much lower activity in the 573 – 723 K temperature region for this sample compare to $Co_{2.0}$SiBEA indicates that extra-framework cobalt species present in $Co_{2.0}$HAlBEA are less active sites in SCR of NO with ammonia than isolated framework mononuclear cobalt(II) present in $Co_{2.0}$SiBEA.

As shown in **Figure 9** for all studied catalysts the formation of N_2O was observed, however at very low level in whole temperature range. The highest nitrous oxide

concentration – 42 ppm – was detected for $Co_{3.0}$SiBEA catalyst at 773 K. This by-product may come from both NH_3 oxidation (reaction (4)) and SCR process itself.

In order to check the occurrence of side ammonia oxidation reaction, the catalytic tests were carried out without NO and the results are presented in **Figure 10**. All catalysts showed poor ability for oxidation of NH_3 into N_2O while for some of them significant amount of NO was detected. The increase in NO formation was observed with the increasing cobalt content. Very high amounts of NO were formed (> 225 ppm at 773 K) when $Co_{3.0}$SiBEA catalyst was applied. With the increase in reaction temperature, the increase of NO concentration in the products was registered. These observations confirm that extra-framework cobalt(II) species present in $Co_{3.0}$SiBEA zeolite are more active in the oxidation of ammonia to nitrogen(II) oxide than in the reduction of NO to N_2 and H_2O in selective catalytic redaction of NO with ammonia. Thus, the sharp decrease of NO conversion in selective catalytic reduction of NO at high temperature was due to the formation of NO as a result of ammonia oxidation and not catalyst deactivation. Similar conclusion was drawn by Chmielarz et al. in their work on cobalt containing hydrotalcite [19]. On the other hand, the catalyst containing predominantly isolated framework mononuclear cobalt(II) species showed high conversion of NO into N_2 with the absence of undesired products.

From the results presented in this work it may be concluded that the application in SCR of NO with ammonia of CoSiBEA zeolite catalysts with predominantly isolated mononuclear Co(II) incorporated into zeolite framework led to several advantages, such as: (i) a very high efficiency of these catalysts at a wide temperature range (573 – 773), (ii) a higher activity of CoSiBEA catalysts with low Co content than other Co-containing catalyst with much higher Co content [12,16,19], and (iii) the absence of hazardous side-product (N_2O).

Conclusions

XPS, DR UV-Vis and FTIR studies revealed that in Co_xSiBEA catalysts with 2 or less Co wt %, prepared by the two-step postsynthesis method, cobalt occurs as isolated mononuclear Co(II) incorporated into zeolite framework. On the other hand, $Co_{3.0}SiBEA$ catalyst contains a mixture of framework and extra-framework Co(II) species.

Pyridine sorption followed by FTIR experiments allowed to establish that the incorporation of cobalt into zeolite framework resulted in the formation of new Lewis acidic sites with moderate strength.

The application of Co_xSiBEA zeolites with predominantly isolated mononuclear Co(II) as catalyst of selective catalytic reduction of NO with ammonia led to high NO conversion at the wide temperature range, with the maximum of 79% at 673 K for $Co_{2.0}SiBEA$.

$Co_{3.0}SiBEA$ containing the mixture of framework and extra-framework cobalt species was inactive in NH_3-SCR process at high temperature range because of the preferential ammonia oxidation to NO.

For all catalysts negligible formation of N_2O was found.

Acknowledgment

This project was funded by the National Science Center “PRELUDIUM” UMO-2012/07/N/ST5/00171 (R.B., S.D.).

References

[1] C. He, Y. Wang, Y. Cheng, C.K. Lambert, R.T. Yang,

Appl. Catal. A Gen. 368 (2009)121.

[2] A. Sultana, M. Sasaki, H. Hamada, Catal. Today 185 (2012) 284.

[3] S.S.R. Putluru, A. Riisager, R. Fehrmann, Appl. Catal. B Environ. 97 (2010) 333.

[4] I. Lezcano-Gonzalez, U. Deka, H.E. van der Bij, P. Paalanen, B. Arstad, B.M.

Weckhuysen, a. M. Beale, Appl. Catal. B Environ. 154-155 (2014) 339.

[5] M. Motak, Catal. Today 137 (2008) 247.

[6] J. Klinik, B. Samojeden, T. Grzybek, W. Suprun, H. Papp, R. Gläser,

Catal. Today 176 (2011) 303.

[7] R. Baran, T. Onfroy, T. Grzybek, S. Dzwigaj,

Appl. Catal. B 136-137 (2013) 186.

[8] S. Sitshebo, A. Tsolakis, K. Theinnoi, Int. J. Hydrogen Energy 34 (2009) 7842.

[9] J. Janas, J. Gurgul, R.P. Socha, S. Dzwigaj, Appl. Catal. B Environ. 91 (2009) 217.

[10] C. Thomas, Appl. Catal. B Environ. 162 (2015) 454.

[11] L. Righini, L. Kubiak, S. Morandi, L. Castoldi, L. Lietti, P. Forzatti,

ACS Catal. 4 (2014) 3261.

[12] F. Bin, C. Song, G. Lv, J. Song, X. Cao, H. Pang, K. Wang,

J. Phys. Chem. C 116 (2012) 26262.

[13] J. Janas, T. Machej, J. Gurgul, R.P. Socha, M. Che, S. Dzwigaj,

Appl. Catal. B Environ. 75 (2007) 239.

[14] S.-J. Jong, S. Cheng, Appl. Catal. A Gen. 126 (1995) 51.

[15] C. Montes de C, A. Luz Villa de P, M.. Ramírez-Corredores,

Appl. Catal. A 197 (2000) 151.

[16] R. Moreno-Tost, J. Santamaría-González, P. Maireles-Torres, E. Rodríguez-Castellón,

A. Jiménez-López, Appl. Catal. B Environ. 38 (2002) 51.

[17] R. Moreno-Tost, J. Santamaría-González, E. Rodríguez-Castellón, A. Jiménez-López,

Appl. Catal. B Environ. 52 (2004) 241.

[18] M. Brandhorst, J. Zajac, D.J. Jones, J. Rozière, M. Womes, a. Jimenez-López, E.

Rodríguez-Castellón, Appl. Catal. B Environ. 55 (2005) 267.

[19] L. Chmielarz, P. Kuśtrowski, A. Rafalska-Łasocha, D. Majda, R. Dziembaj,

Appl. Catal. B Environ. 35 (2002) 195.

[20] F. Lónyi, H.E. Solt, Z. Pászti, J. Valyon, Appl. Catal. B Environ. 150-151 (2014) 218.

[21] F. Lónyi, H.E. Solt, J. Valyon, A. Boix, L.B. Gutierrez,

J. Mol. Catal. A Chem. 345 (2011) 75.

[22] R. Baran, T. Onfroy, S. Casale, S. Dzwigaj, J. Phys. Chem. C 118 (2014) 20445.

[23] R. Baran, Y. Millot, T. Onfroy, J.M. Krafft, S. Dzwigaj,

Microporous Mesoporous Mater. 163 (2012) 122.

[24] A. Śrębowata, R. Baran, I.I. Kamińska, T. Onfroy, J.-M. Krafft, S. Dzwigaj,

Catal.Today 251 (2015) 73.

[25] C.A. Emeis, J. Catal. 141 (1993) 347.

[26] M. Trombetta, G. Busca, L. Storaro, M. Lenarda, M. Casagrande, A. Zambon,

Phys.Chem. Chem. Phys. 2 (2000) 3529.

[27] Y. Gong, T. Dou, S. Kang, Q. Li, Y. Hu, Fuel Process. Technol. 90 (2009) 122.

[28] R. Baran, Y. Millot, T. Onfroy, F. Averseng, J.-M. Krafft, S. Dzwigaj,

Microporous Mesoporous Mater. 161 (2012) 179.

[29] A. Petushkov, G. Merilis, S.C. Larsen, Microporous Mesoporous Mater. 143 (2011) 97.

[30] J.C. Groen, S. Abelló, L. a. Villaescusa, J. Pérez-Ramírez, Microporous Mesoporous

Mater. 114 (2008) 93.

[31] Q.-H. Xia, S.-C. Shen, J. Song, S. Kawi, K. Hidajat, J. Catal. 219 (2003) 74.

[32] C. Yang, Q. Xu, Zeolites 19 (1997) 404.

[33] R. Dimitrova, G. Gunduz, L. Dimitrov, T. Tsoncheva, S. Yialmaz, E. a. Urquieta Gonzalez, J. Mol. Catal. A Chem. 214 (2004) 265.

[34] G. Prieto, A. Martínez, P. Concepción, R. Moreno-Tost, J. Catal. 266 (2009) 129.

[35] C. Chupin, a. C. van Veen, M. Konduru, J. Després, C. Mirodatos, J. Catal. 241 (2006) 103.

[36] P. Selvam, S. Mohapatra, J. Catal. 233 (2005) 276.

[37] M. Kato, T. Ikeda, T. Kodaira, S. Takahashi, Microporous Mesoporous Mater. 142 (2011) 444.

[38] L. Zhang, L. Dong, W. Yu, L. Liu, Y. Deng, B. Liu, H. Wan, F. Gao, K. Sun, L. Dong, J. Colloid Interface Sci. 355 (2011) 464.

[39] J. Liu, Z. Zhao, J. Wang, C. Xu, A. Duan, G. Jiang, Q. Yang, Appl. Catal. B Environ.84 (2008) 185.

[40] A. Boix, E.E. Miró, E.A. Lombardo, M.A. Banares, R. Mariscal, J.L.G. Fierro, J. Catal.217 (2003) 186.

[41] L.P. Oleksenko, Theor. Exp. Chem. 40 (2004) 331.

[42] T.L. Barr, J. Vac. Sci. Technol. A Vacuum, Surfaces, Film. 9 (1991) 1793.

[43] H.-H. Chen, S.-C. Shen, X. Chen, S. Kawi, Appl. Catal. B Environ. 50 (2004) 37.

[44] A. Śrebowata, R. Baran, D. Łomot, D. Lisovytskiy, T. Onfroy, S. Dzwigaj, Appl. Catal. B Environ. 147 (2014) 208.

[45] K. Hadjiivanov, E. Ivanova, R. Kefirov, J. Janas, A. Plesniar, S. Dzwigaj, M. Che, Microporous Mesoporous Mater. 131 (2010) 1.

[46] K. Hadjiivanov, B. Tsyntsarski, T. Venkov, M. Daturi, J. Saussey, J.-C. Lavalley, Phys.Chem. Chem. Phys. 5 (2002) 243.

[47] K. Hadjiivanov, B. Tsyntsarski, T. Venkov, D. Klissurski, M. Daturi, J. Saussey, J.-C. Lavalley, Phys. Chem. Chem. Phys. 5 (2003) 1695.

[48] A. Mihaylova, K. Hadjiivanov, S. Dzwigaj, M. Che, J. Phys. Chem. B 110 (2006) 19530.

[49] E. Ivanova, K. Hadjiivanov, S. Dzwigaj, M. Che, Microporous Mesoporous Mater. 89 (2006) 69.

Table 1. Chemical composition of BEA samples.

Sample	Concentration (wt %)			Ratio	
	Co	Si	Al	Si/Al	Co/Si
TEABEA	-	44.2	2.649	17	-
HAlBEA	-	44.25	2.245	20	-
$Co_{2.0}$HAlBEA	2.21	42.9	2.143	20	0.052
SiBEA	-	42.49	0.028	>1000	-
$Co_{1.0}$SiBEA	1.12	45.54	0.037	>1000	0.024
$Co_{2.0}$SiBEA	2.16	44.8	0.037	>1000	0.048
$Co_{3.0}$SiBEA	3.63	42.91	0.024	>1000	0.085

Table 2. Structural properties of BEA samples.

Sample	2θ (◦)	d_{302} (Å)	XRD relative intensity (%)
TEABEA	22.326	3.9788	100
HAlBEA	22.493	3.9497	88
$Co_{2.0}$HAlBEA	22.447	3.9576	86
SiBEA	22.662	3.9206	70
$Co_{2.0}$SiBEA	22.536	3.9421	58
spent-$Co_{2.0}$SiBEA	22.460	3.9553	64
$Co_{3.0}$SiBEA	22.530	3.9432	59
spent-$Co_{3.0}$SiBEA	22.531	3.9437	58

Table 3. Textural properties of HAlBEA, $Co_{2.0}$HAlBEA, SiBEA and $Co_{1.0}$SiBEA.

Samples	Specific surface area S_{BET}, (m^2 g^{-1})	Micropores volume V_{mic}, (mL g^{-1})	Total pore volume V_{tot}, (mL g^{-1})	Average pores diameter D, (nm)
HAlBEA	641	0.26	0.38	2.67
$Co_{2.0}$HAlBEA	577	0.23	0.39	2.89
SiBEA	612	0.25	0.37	2.64
$Co_{1.0}$SiBEA	613	0.25	0.38	2.76

Table 4. XPS chemical analysis of C-$Co_{1.0}$SiBEA, C-$Co_{3.0}$SiBEA and C-$Co_{2.0}$HAlBEA .

Sample	Composition (at. %)					Ratio	
	Si 2p	O 1s	C 1s	Al 2p	Co 2p	Co/Si	Si/Al
C-$Co_{1.0}$SiBEA	29.7	55.13	14.99	-*	0.18	0.006	-
C-$Co_{3.0}$SiBEA	29.26	55.89	14.43	-	0.42	0.014	-
C-$Co_{2.0}$HAlBEA	28.81	55.48	13.88	1.51	0.32	0.011	19.08

* - aluminum was not detected

Table 5. The amounts of Brønsted and Lewis acidic centers in SiBEA, $Co_{2.0}$SiBEA and $Co_{3.0}$SiBEA.

Type of acidic centers	Temp.(K)	Sample				
		HAlBEA	$Co_{2.0}$HAlBEA	SiBEA	$Co_{2.0}$SiBEA	$Co_{3.0}$SiBEA
Brønsted acidic centers (μmol g^{-1})	423	334	130	15	15	8
	573	239	58	8	0	0
Lewis acidic centers (μmol g^{-1})	423	136	352	2	177	159
	573	137	268	1	111	91

Figure Captions

Figure 1. XRD patterns recorded at room temperature of TEABEA, HAlBEA, $Co_{2.0}$HAlBEA, SiBEA, $Co_{2.0}$SiBEA and $Co_{3.0}$SiBEA.

Figure 2. FTIR spectra recorded at ambient atmosphere of TEABEA, HAlBEA, SiBEA, and C-$Co_{2.0}$SiBEA in skeleton vibrations range.

Figure 3. DR UV–vis spectra recorded at ambient atmosphere of C-$Co_{2.0}$SiBEA and C-$Co_{3.0}$SiBEA

Figure 4. XPS spectra recorded at room temperature of Co 2p core level of C-$Co_{1.0}$SiBEA, C-$Co_{3.0}$SiBEA and C-$Co_{2.0}$HAlBEA.

Figure 5. FTIR spectra recorded at room temperature of SiBEA, $Co_{2.0}$SiBEA and $Co_{3.0}$SiBEA after adsorption of pyridine (133 Pa) for 1 h at room temperature and desorption at 423 K for 1 h.

Figure 6. FTIR difference spectra in carbonyl (A) and hydroxyl (B) stretching regions of $Co_{2.0}$SiBEA after adsorption of a small dose (ca. 10 μmol g^{-1} (a–d) then 45 μmol g^{-1} (e–f) of CO at 100 K.

Figure 7. FTIR spectra of CO (267 Pa equilibrium pressure) adsorbed at 100 K on C-$Co_{2.0}$SiBEA and evolution of the spectra in dynamic vacuum at 100 K (a–g); carbonyl (A) and hydroxyl (B) stretching regions.

Figure 8. NO conversion in SCR of NO with NH_3 on HAlBEA, $Co_{2.0}$HAlBEA, SiBEA, $Co_{1.0}$SiBEA, $Co_{2.0}$SiBEA and $Co_{3.0}$SiBEA.

Figure 9. N_2O formation in SCR of NO with NH_3 on SiBEA, $Co_{1.0}$SiBEA, $Co_{2.0}$SiBEA $Co_{3.0}$SiBEA and $Co_{2.0}$HAlBEA.

Figure 10 NO and N_2O formation in NH_3 oxidation on $Co_{2.0}$SiBEA and $Co_{3.0}$SiBEA.

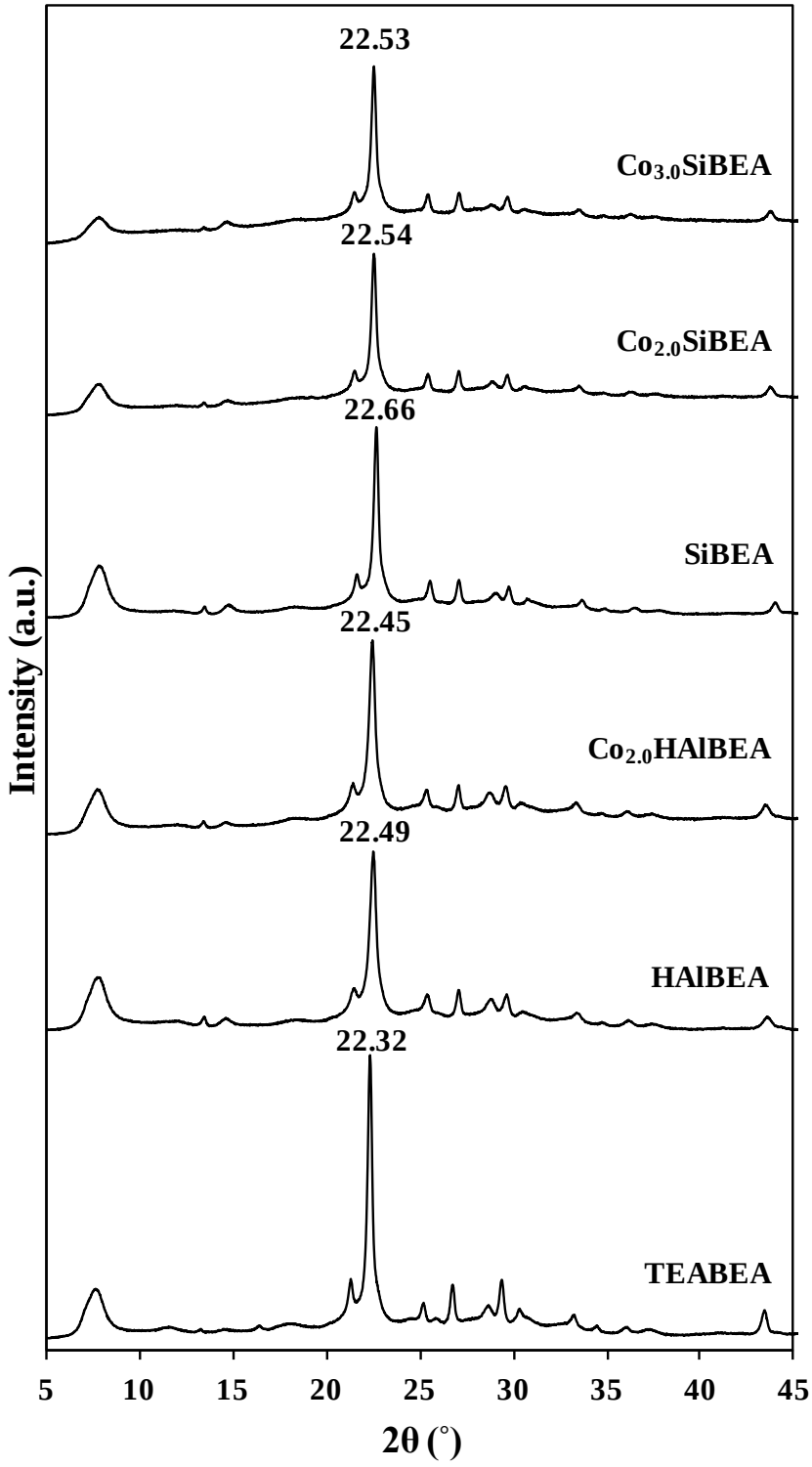
22.53
Co3.0SiBEA
22.54
Co2.0SiBEA
22.66
SiBEA
22.45
Co2.0HAlBEA
22.49
HAlBEA
22.32
TEABEA
Intensity (a.u.)
5
10
15
20
25
30
35
40
45
2θ (°)

Figure 1

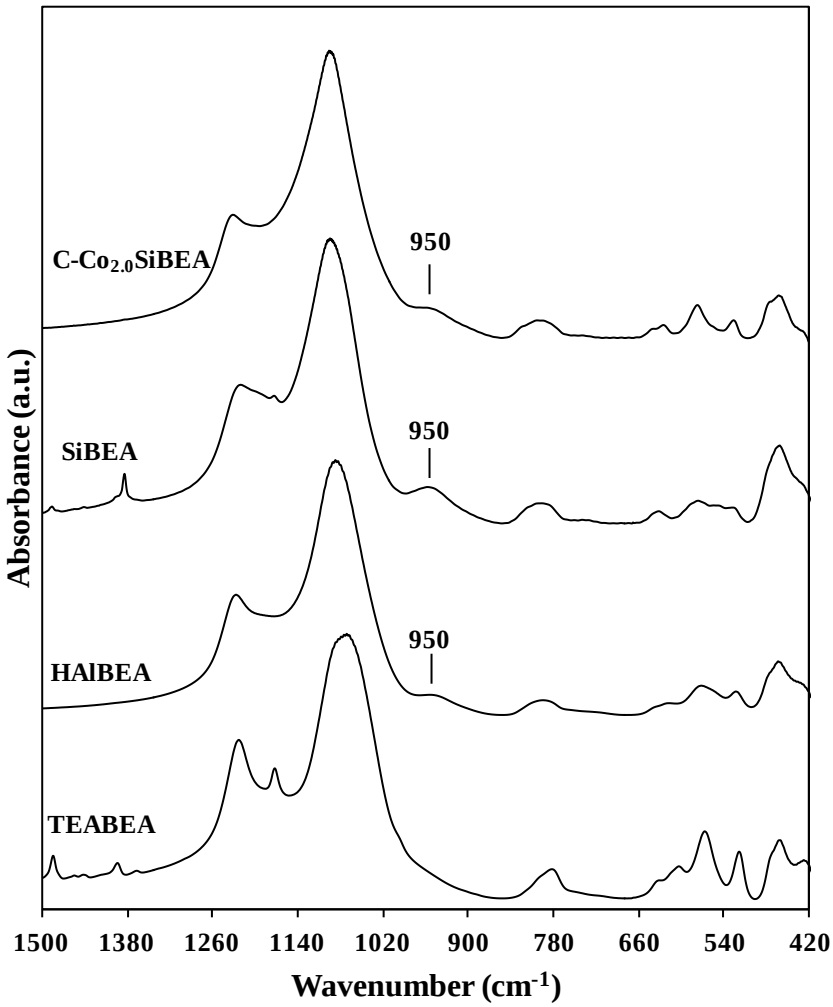
C-Co2.0SiBEA
SiBEA
HAlBEA
TEABEA
950
950
950
Absorbance (a.u.)
1500
1380
1260
1140
1020
900
780
660
540
420
Wavenumber (cm-1)

Figure 2

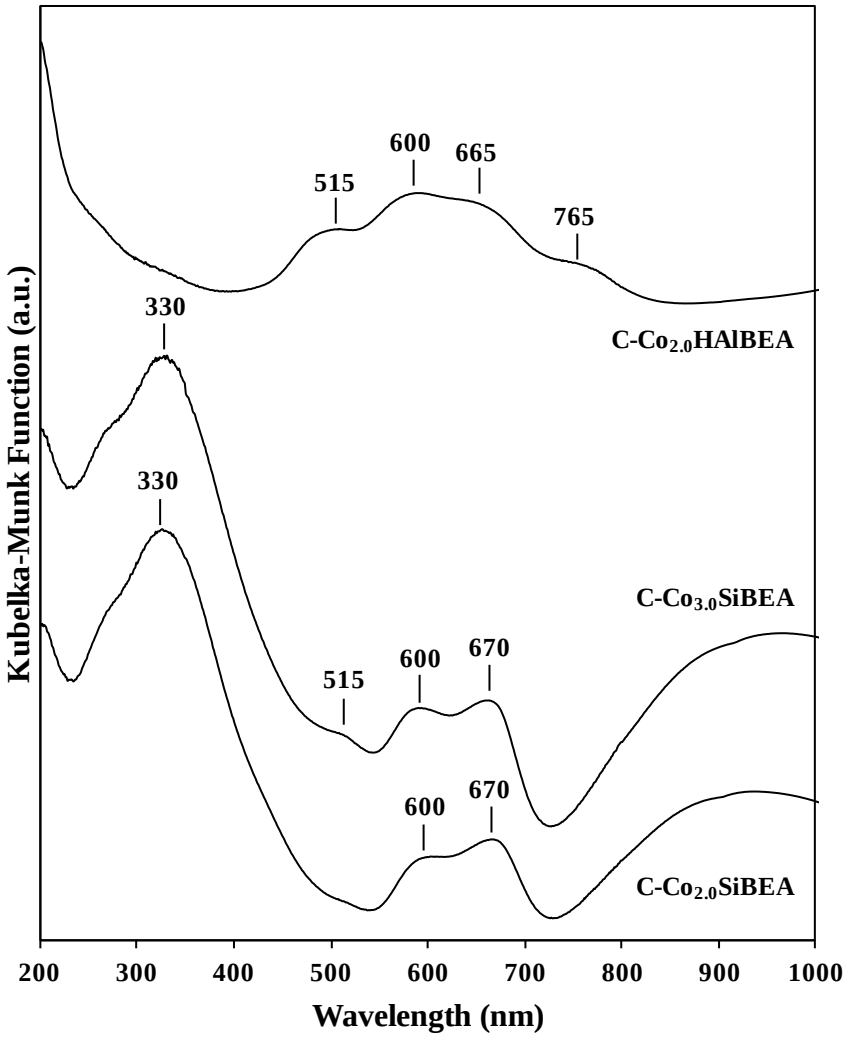
Kubelka-Munk Function (a.u.)
Wavelength (nm)
200
300
400
500
600
700
800
900
1000
515
600
665
765
C-Co2.0HAlBEA
330
330
C-Co3.0SiBEA
515
600
670
600
670
C-Co2.0SiBEA

Figure 3

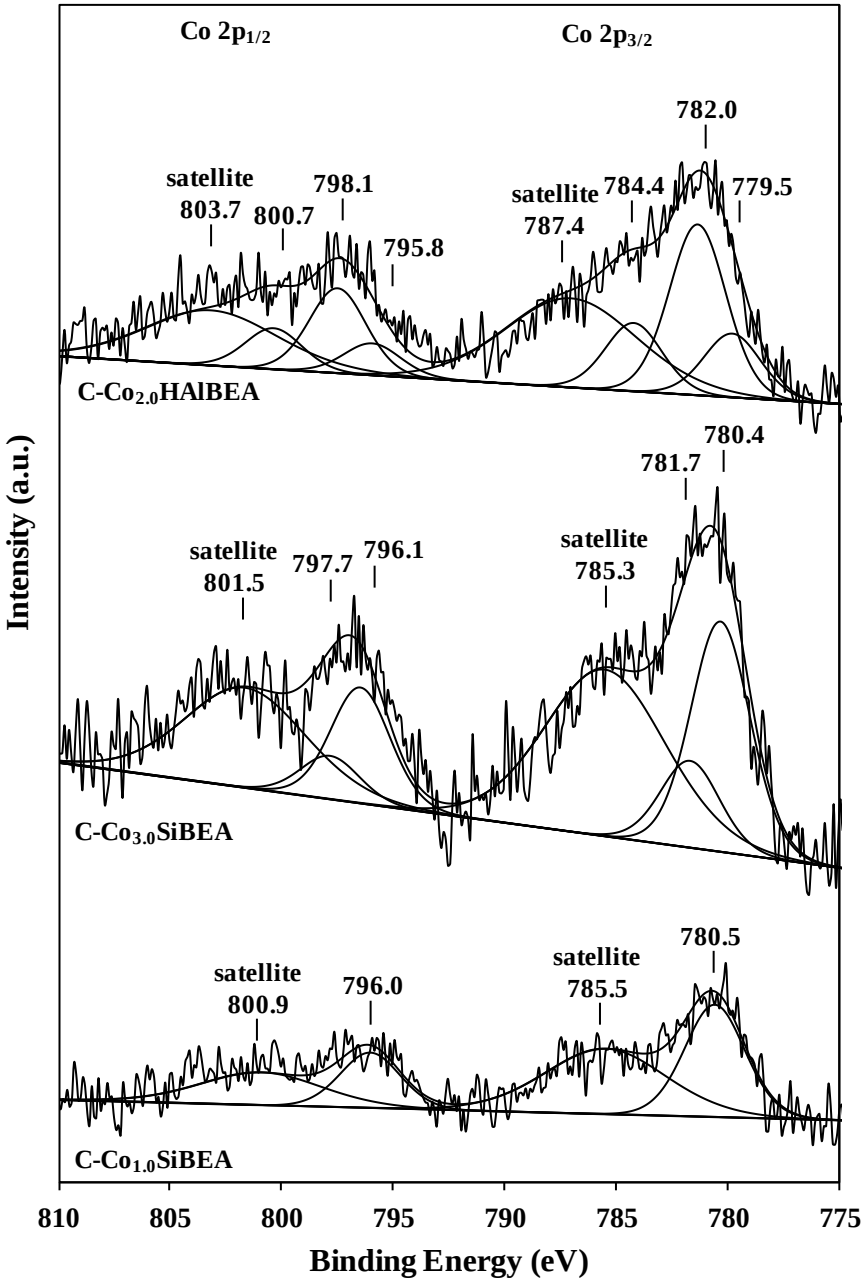
Co 2p1/2
Co 2p3/2
782.0
satellite
803.7
800.7
798.1
795.8
satellite
787.4
784.4
779.5
C-Co2.0HAlBEA
780.4
781.7
satellite
801.5
797.7
796.1
satellite
785.3
C-Co3.0SiBEA
780.5
satellite
800.9
796.0
satellite
785.5
C-Co1.0SiBEA
Intensity (a.u.)
810
805
800
795
790
785
780
775
Binding Energy (eV)

Figure 4

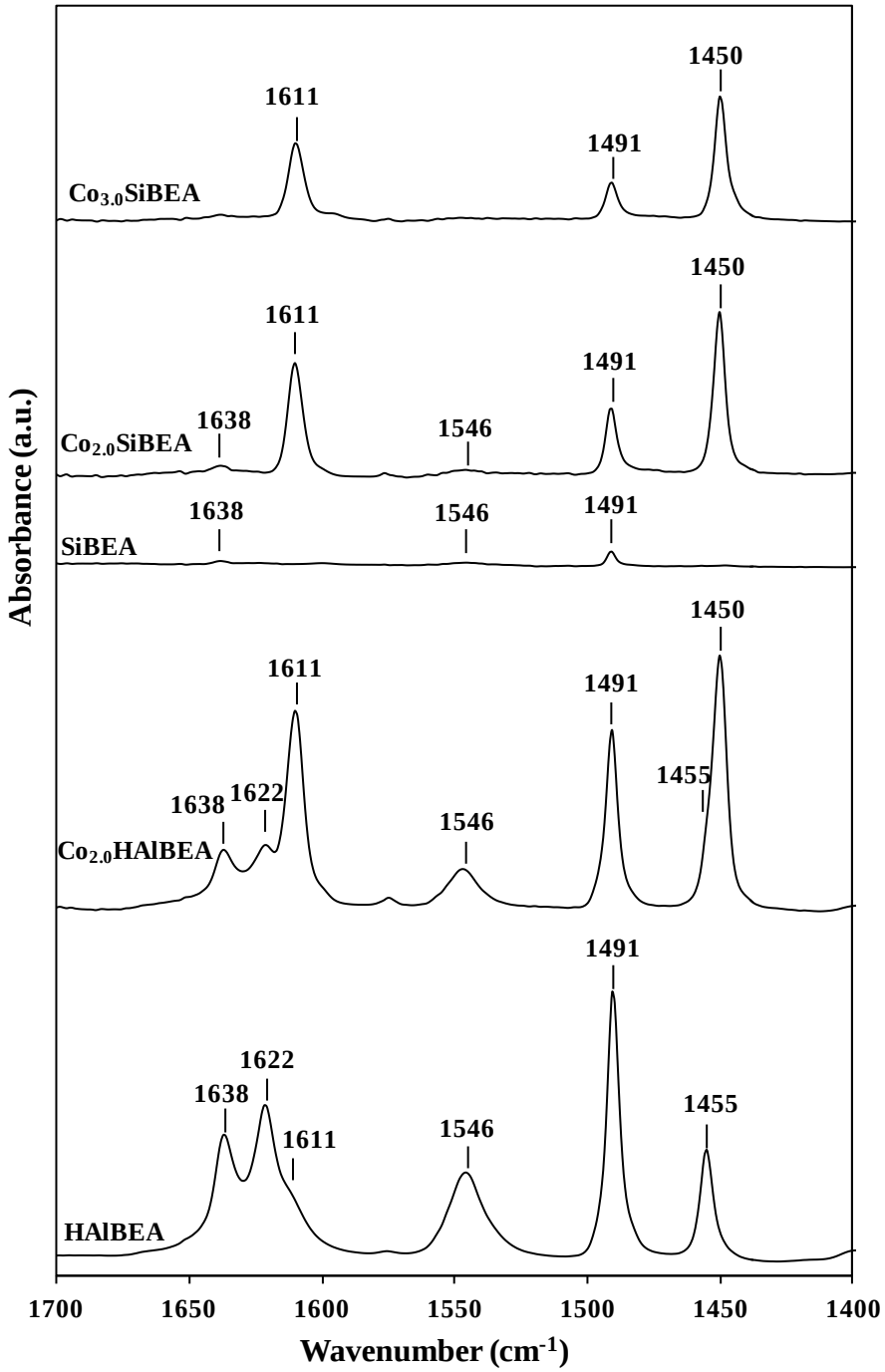
Absorbance (a.u.)
Co3.0SiBEA
1611
1491
1450
Co2.0SiBEA
1638
1546
SiBEA
Co2.0HAlBEA
1622
1455
HAlBEA
1700
1650
1600
1550
1500
1450
1400
Wavenumber (cm-1)

Figure 5

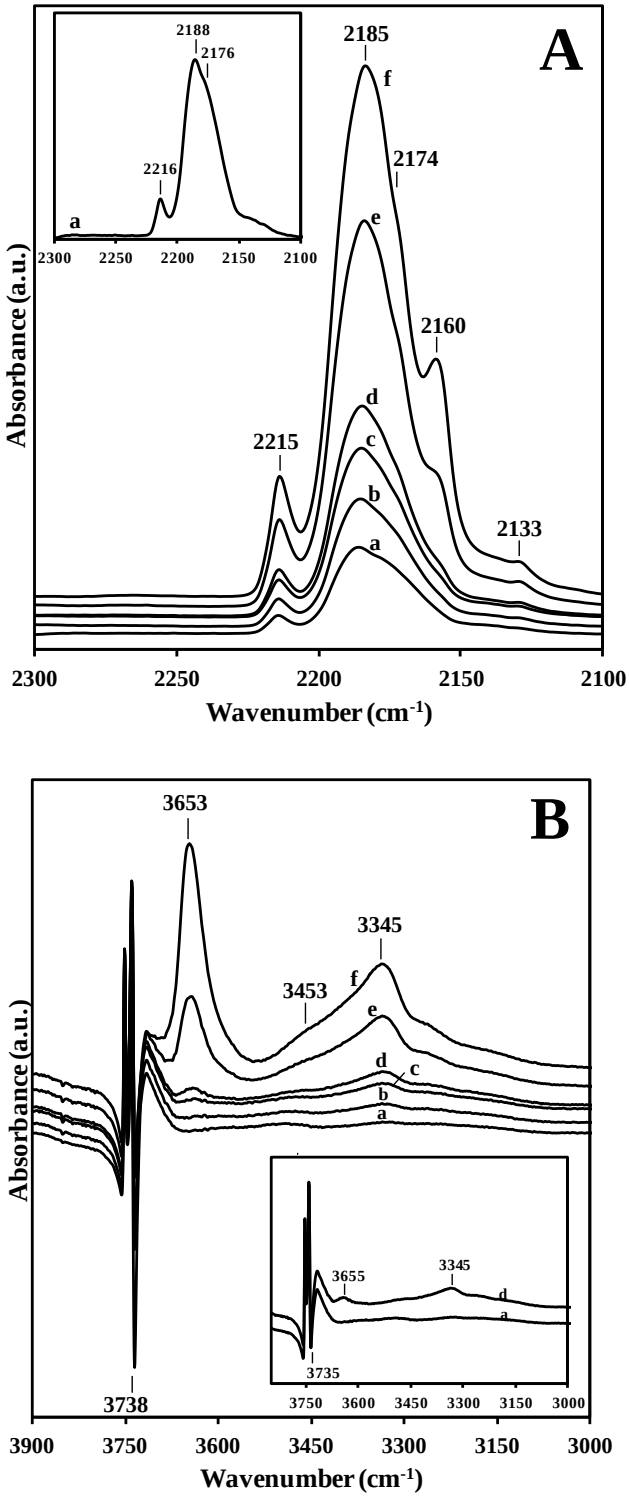
A
2185
f
2174
e
2160
d
c
b
a
2215
2133
2188
2176
2216
a
2300
2250
2200
2150
2100
Absorbance (a.u.)
Wavenumber (cm-1)
B
3653
3345
3453
f
e
d
c
b
a
3738
3655
3345
d
a
3735
3750
3600
3450
3300
3150
3000
3900
Absorbance (a.u.)
Wavenumber (cm-1)

Figure 6

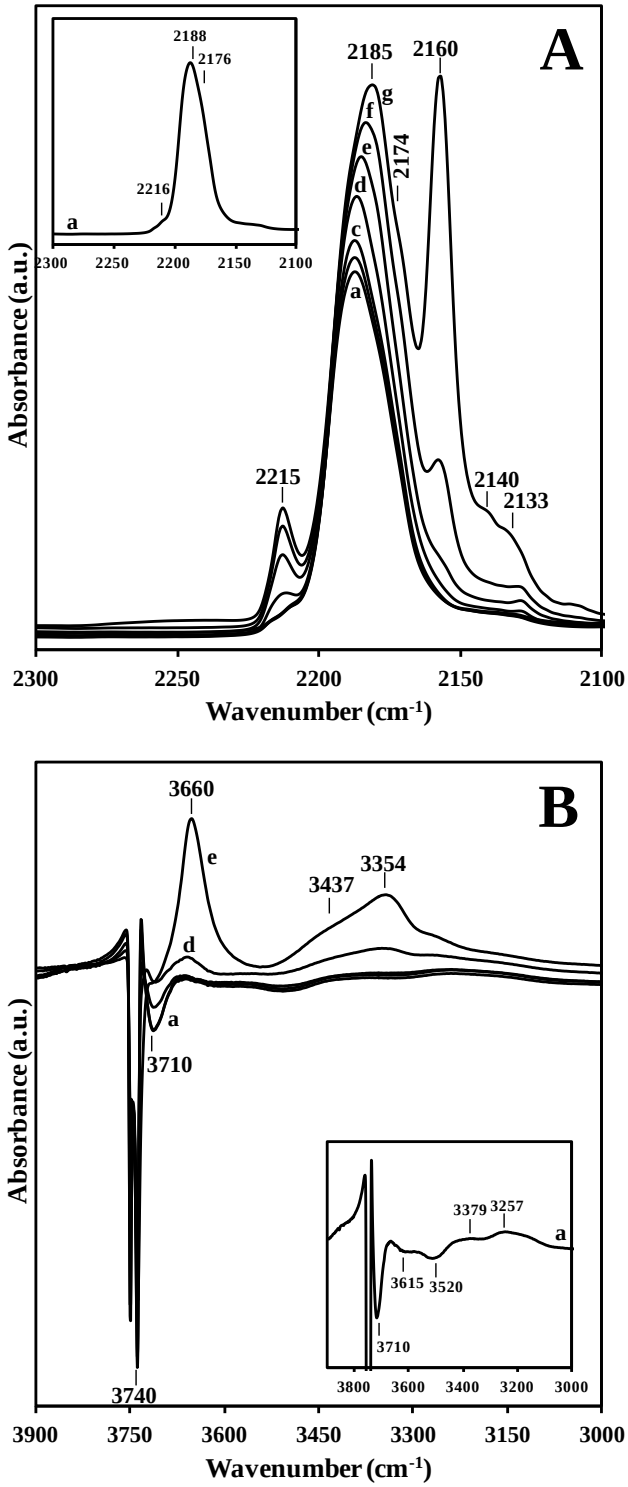
A
2188
2176
2216
a
2300 2250 2200 2150 2100
2185
2160
g
f
e
2174
d
c
a
2215
2140
2133
Absorbance (a.u.)
2300 2250 2200 2150 2100
Wavenumber (cm-1)
B
3660
e
3354
3437
d
a
3710
3740
3379 3257
a
3615 3520
3710
3800 3600 3400 3200 3000
3900 3750 3600 3450 3300 3150 3000
Absorbance (a.u.)
Wavenumber (cm-1)

Figure 7

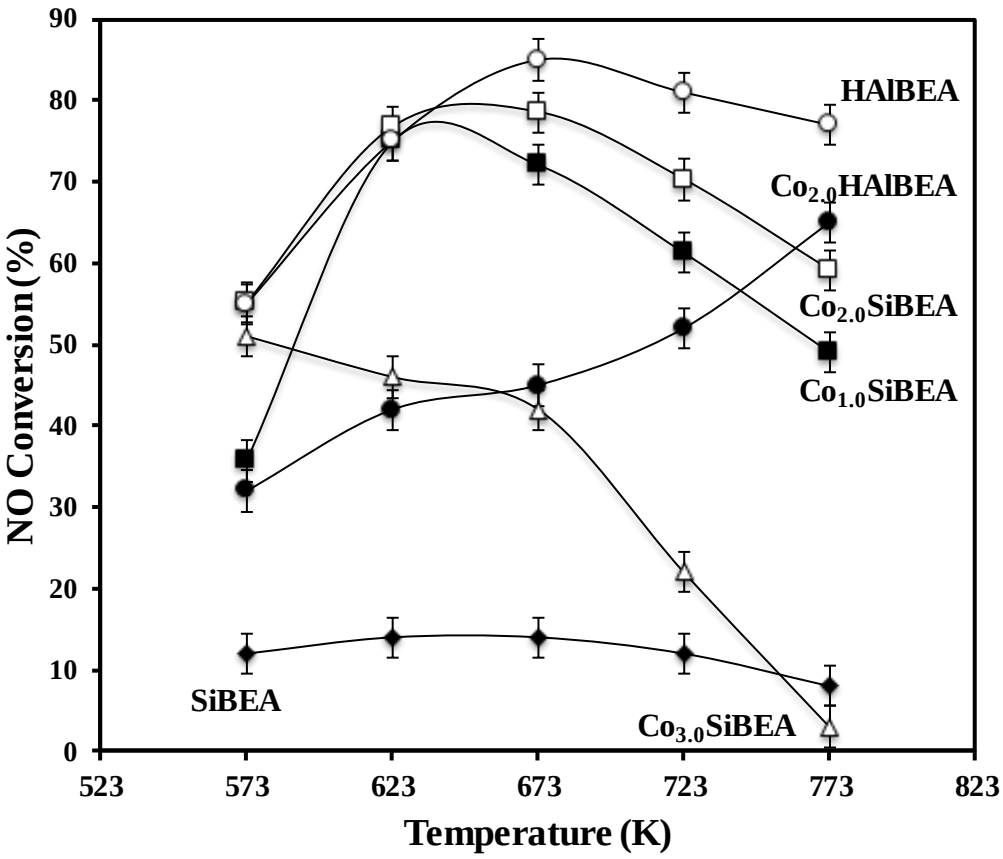
NO Conversion (%)
Temperature (K)
HAlBEA
Co2.0HAlBEA
Co2.0SiBEA
Co1.0SiBEA
Co3.0SiBEA
SiBEA
90
80
70
60
50
40
30
20
10
0
523
573
623
673
723
773
823

Figure 8

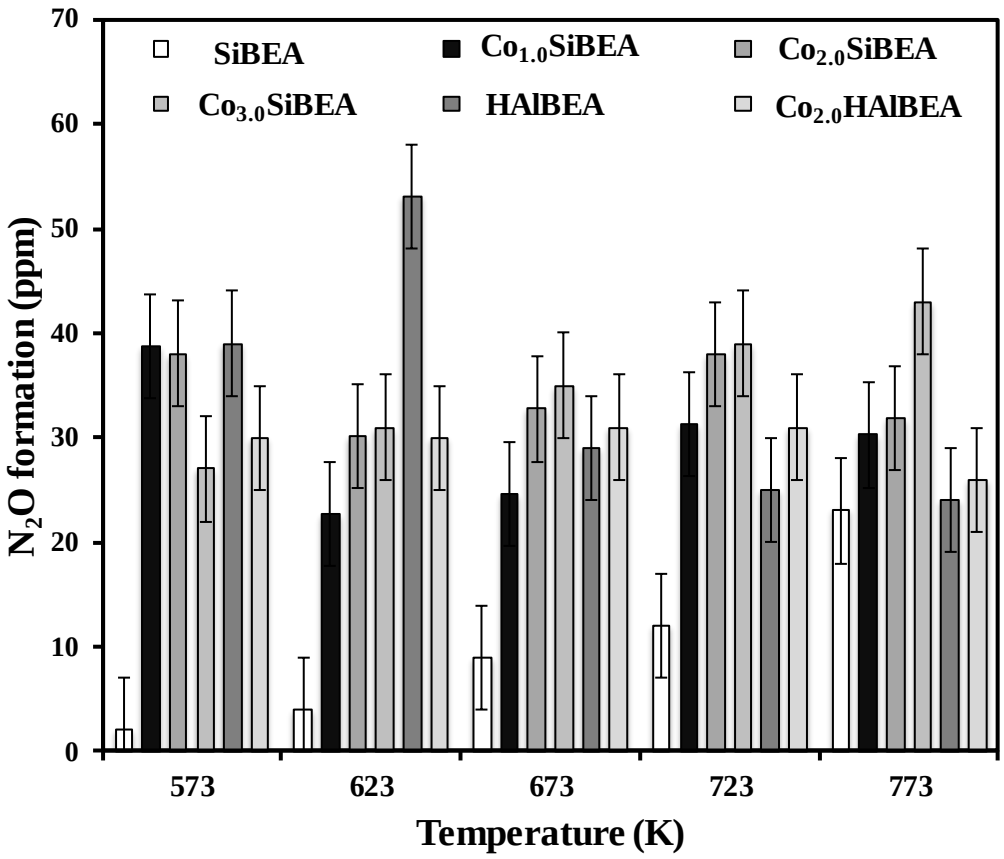
SiBEA
Co1.0SiBEA
Co2.0SiBEA
Co3.0SiBEA
HAlBEA
Co2.0HAlBEA
N2O formation (ppm)
0
10
20
30
40
50
60
70
573
623
673
723
773
Temperature (K)

Figure 9

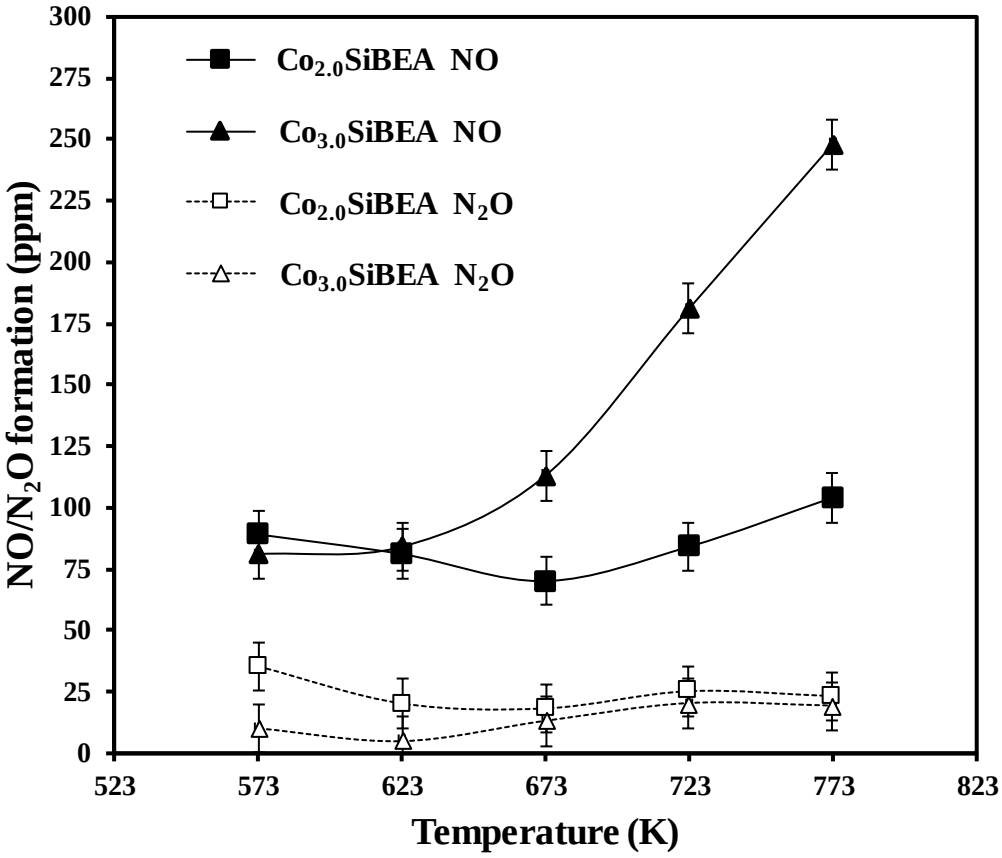
Co2.0SiBEA NO
Co3.0SiBEA NO
Co2.0SiBEA N2O
Co3.0SiBEA N2O
NO/N2O formation (ppm)
Temperature (K)
300
275
250
225
200
175
150
125
100
75
50
25
0
523
573
623
673
723
773
823

Figure 10